

See discussions, stats, and author profiles for this publication at: <https://www.researchgate.net/publication/343615641>

Development of Non-Invasive Monitoring Approach to Diagnose Leaks in Liquid Pipelines

Article in *Technology Reports of Kansai University* · July 2020

CITATIONS

0

READS

48

4 authors:



Javier Jiménez-Cabas

Corporación Universidad de la Costa

21 PUBLICATIONS 44 CITATIONS

[SEE PROFILE](#)



Lizeth Torres

Universidad Nacional Autónoma de México

85 PUBLICATIONS 522 CITATIONS

[SEE PROFILE](#)



Francisco-Ronay López-Estrada

Instituto Tecnológico de Tuxtla Gutiérrez

79 PUBLICATIONS 376 CITATIONS

[SEE PROFILE](#)



Ildeberto Santos-Ruiz

Tecnologico Nacional de Mexico

16 PUBLICATIONS 51 CITATIONS

[SEE PROFILE](#)

Some of the authors of this publication are also working on these related projects:



Leak detection in pipelines [View project](#)



Special Issue: Optimization for Control, Observation and Safety. Journal Processes (ISSN 2227-9717). JCR IF: 1.963 [View project](#)

Development of Non-Invasive Monitoring Approach to Diagnose Leaks in Liquid Pipelines

Javier Jiménez-Cabas^{1*}, Lizeth Torres², Francisco-Ronay López-Estrada³, Ildeberto Santos-Ruiz³,

Fabián Manrique-Morelos⁴

Departamento de Ciencias de la Computación y Electrónica, Universidad de la Costa, Barranquilla, Atlántico, Colombia¹

Instituto de Ingeniería, Universidad Nacional Autónoma de México, Ciudad de México, Distrito Federal, México²

Departamento de Electrónica, Instituto Tecnológico de Tuxtla Gutiérrez, Tuxtla Gutiérrez, Chiapas, México³

Departamento de Innovación, Indutronica del Caribe S.A.S., Barranquilla, Atlántico, Colombia⁴

* Corresponding author: jjimenez41@cuc.edu.co

Abstract— This paper presents a novel non-invasive monitoring method, based on a Liénard-type model (LTM) to diagnose single and sequential leaks in liquid pipelines. The LTM describes the fluid behavior in a pipeline and is given only in terms of the flow rate. Our method was conceived to be applied in pipelines mono-instrumented with flowmeters or in conjunction with pressure sensors that are temporarily unavailable. The approach conception starts with the discretization of the LTM spatial domain into a prescribed number of sections. Such discretization is performed to obtain a lumped model capable of providing a solution (an internal flow rate) for every section. From this lumped model, a set of algebraic equations (known as residuals) are deduced as the difference between the internal discrete flows and the nominal flow (the mean of the flow rate calculated before the leak). Once the residuals are calculated a principal component analysis (PCA) is carried out to detect a leak occurrence. In the presence of a leak, the residual closest to zero will indicate the section where a leak is occurring. Some simulation-based tests in PipelineStudio® and experimental tests in a lab-pipeline illustrating the suitability of our method are shown at the end of this article.

Keywords— Leak diagnosis in pipelines, Non-invasive monitoring method, Liénard-type model.

1. Introduction

Pipeline networks are the most efficient mode of transportation for fluid products as gasoline, diesel, jet fuel, home heating oil, raw natural gas liquids, among others. As a long-distance transport mean, pipelines have to fulfill high demands of safety and reliability. Thus, owners and operators of pipeline systems are subject to stringent operational safety regulations, in addition to increased pressure from environmental organizations. Although pipelines are designed and built to maintain their integrity, the occurrence of leakages in pipeline systems is unfortunately very common events; whereby every pipeline operation should incorporate a leak monitoring system (LMS).

There are different methods for leak monitoring which, according to the American Petroleum Institute [1], can be externally based LMS or internally based LMS. The first ones use a specific set of field instrumentation (e.g., sensing cables [2], [3], acoustic sensors [4], laser sensors [5], vapor sensors [6], fiber-optic cables [7],

infrared radiometers or thermal cameras [8]) to monitor external pipeline parameters. While the latter use field instrumentation (e.g., flow or pressure sensors [9], [10]) to monitor internal pipeline parameters. Because of the high costs associated with installing and maintaining sensors and communication equipment for the entire length of the pipeline, external methods are typically used only in very special cases. On the other hand, internal methods are constituted as most practical to diagnose significant leaks early and reliably from a remote location. The methods based on mathematical models [11]–[14] and the analysis of the pressure wave [15], [16] classify as internal methods. Depending on the circumstances, each of these techniques has its advantages and disadvantages, and no single method can always meet operational needs.

Despite great advances in leak monitoring systems, according to the pipeline incident reports of the Pipeline and Hazardous Materials Safety Administration (PHMSA), trends in the last 20 years do not show a reduction in the number of pipeline incidents associated to leaks (see Table 1, [17]). This suggests that pipeline leak detection is an open problem.

Bearing this in mind, in this work, it is proposed a non-invasive monitoring method to diagnose (i.e., to detect and locate) pipeline leaks by only using flow rate measures. Usually, flow rates have only been employed to compute a mass balance that allows the leak detection but not the leak location [18], [19]. From a commonsense perspective, it is profitable to utilize pressure sensors to monitor leaks since they are less expensive and easier to install [20]. Our strategy was intended to be utilized to complement the monitoring made with another sort of techniques, and not to supplant or contend with leak detection strategies using pressure sensors, for example, the negative pressure wave techniques [21], the wave reflection strategies, the pressure point analysis strategies [22] or the gradient strategies [23], [24].

Table 1. PHMSA pipeline incidents: (1999-2018).

Year	Number	Fatalities	Injuries	Total Cost Current Year Dollars
1999	275	22	108	\$185.011.171
2000	290	38	81	\$267.337.902
2001	233	7	61	\$82.057.318
2002	258	12	49	\$129.249.925
2003	297	12	71	\$170.240.455
2004	309	23	56	\$326.569.088
2005	336	16	46	\$1.533.563.779
2006	257	19	34	\$163.304.539
2007	265	15	46	\$154.031.564
2008	279	8	54	\$615.207.450
2009	275	13	62	\$187.495.748
2010	264	19	103	\$1.924.162.961
2011	285	11	50	\$464.076.405
2012	255	10	54	\$243.140.542
2013	303	8	42	\$389.415.960
2014	302	19	94	\$329.012.567
2015	329	9	48	\$357.431.842
2016	309	16	86	\$331.105.735
2017	302	7	33	\$251.246.673
2018	284	8	92	\$970.869.813
Total Amount	5.707	292	1.270	\$9.074.531.438

The proposed approach is based on the so-called flow-based Liénard form [25], [26]. The finite difference method is used to obtain a lumped parameter version of this Liénard type model, which is implemented in MATLAB® by considering as boundary conditions the inlet and outlet flow rates of the monitored pipeline. The lumped model allows calculating the flow rate for each section in which the pipeline was divided. Unlike what happens when a leak takes place, in the absence of leaks all flow rates given by the model will be equivalent. The residuals corresponding to each section are calculated by subtracting the corresponding flow rate from the pipeline flow rate without leaks; let's call it nominal flow rate. After the residuals are determined, a leakage event can be detected by using a principal component analysis (PCA) algorithm. In the presence of a leak, the section in which the leak occurs is that associated with the residual closets to zero.

PipelineStudio® and a laboratory pipeline are used to carry out simulated and experimental tests outlining the appropriateness of our strategy. The paper is sorted out as follows. Section 2 exhibits a compendium of the elements that compose the considered model. Section 3 portrays the proposed technique. Section 4 exhibits the results of simulation and experimental tests and Section 5 presents the conclusions.

2. Considered model

The pipeline model considered here is mainly based on the equations for the conservation of mass and momentum which describe the transient flow in closed conduits. These equations are a set of partial differential equations since the flow rate, and pressure head in transient flow are functions of time as well as space. These equations are usually referred to as the continuity and momentum equations.

2.1 Fluid dynamics equations

By assuming a horizontal pipeline, constant cross-sectional area, slightly compressible fluid, and negligible convective changes in velocity; the pipeline model can be expressed as [27], [28]:

$$\frac{\partial Q(z,t)}{\partial t} + gA_r \frac{\partial H(z,t)}{\partial t} + \frac{f(Q(z,t))}{2\phi A_r} Q(z,t) |Q(z,t)| = 0 \quad (1)$$

$$\frac{\partial H(z,t)}{\partial t} + \frac{b^2}{gA_r} \frac{\partial Q(z,t)}{\partial z} = 0 \quad (2)$$

where (1) and (2) are known as continuity and momentum equation; $z \in [0, L]$ is the spatial coordinate (m), L is the length of the pipe, $t \in [0, \infty)$ is the time (s) coordinates, while $H(z, t)$ and $Q(z, t)$ represent the pressure head (m) and volumetric flow rate (m^3/s). On the other hand, b , g , A_r and ϕ are wave speed in the fluid (m/s), gravitational acceleration (m/s^2), the cross-sectional area of the pipe (m^2), and inside diameter of the pipe (m) respectively. $f(Q(z, t))$ is the Darcy friction factor which depends on the Reynolds number which in turn depends on the flow rate.

In order that PipelineStudio® find a numerical solution for equations (1) and (2), a pair of the following Dirichlet conditions must be imposed at the boundaries of the pipeline: (i) upstream pressure head, $H(0, t) = H_{in}(t)$, (ii) downstream pressure head, $H(L, t) = H_{out}(t)$, (iii) upstream flow rate, $Q(0, t) = Q_{in}(t)$ and (iv) downstream flow rate, $Q(L, t) = Q_{out}(t)$. In this work, the boundary conditions considered for all the simulations in PipelineStudio® are $H_{in}(t)$ and $H_{out}(t)$, and the found solutions are $Q_{in}(t)$ and $Q_{out}(t)$. Measurements of flow

rates and pressure heads at the ends of the laboratory pipeline are denoted with the same nomenclature of the boundary conditions.

2.2 Friction term

Pressure drop estimation due to the flow friction in pipelines can be considered as a crucial task. In a fully developed steady flow in a straight pipe with a uniform inner diameter ϕ and flowing full, the Darcy-Weisbach equation is considered appropriate to determine head loss due to viscous effects in closed pipelines. The Darcy-Weisbach equation has been defined as follows [29]:

$$h_f = f \frac{LU^2}{2g\phi} \tag{3}$$

where h_f is the frictional pressure loss (m), f is the Darcy-Weisbach friction factor, and U is the mean flow velocity (m/s), which can be experimentally measured as the volumetric flow rate Q per unit cross-sectional area A_r .

The friction factor is a function of the Reynolds number Re which in turn is a function of the flow rate and the relative roughness ε/ϕ , which is the ratio of the mean height of roughness ε with respect to the pipe diameter ϕ . The relation among f , the Reynolds number, and the relative roughness is plotted in Fig 1, which is called the Moody diagram or Moody chart [30]. It is one of the most widely accepted and used charts in engineering. Although it is developed for circular pipes, it can also be used for non-circular pipes by replacing the diameter by the hydraulic diameter.

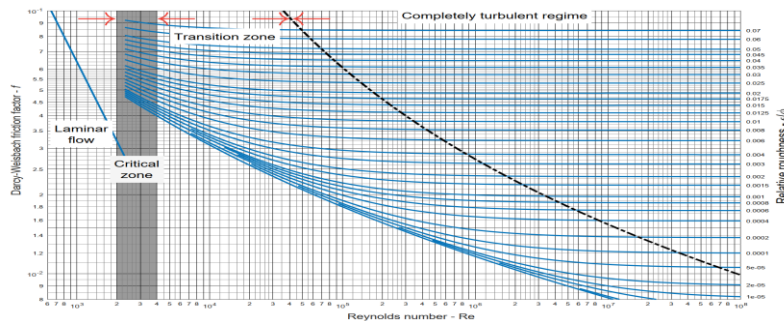


Figure 1. Moody diagram.

Notice that, unlike to transition zone where the flow varies between laminar and complete turbulent flow and the friction factor does not remain constant, at large values of Reynolds number and for a fixed value of relative roughness the friction factor becomes independent of the Reynolds number (complete turbulence zone in Fig 1). An expression for calculating the friction factor for transition and complete turbulent flow, in smooth as well as rough pipes, which agree well with Fig 1 is the relation known as the Colebrook equation given by

$$\frac{1}{\sqrt{f}} = -2 \log \left(\frac{\varepsilon}{3.71\phi} + \frac{2.51}{Re\sqrt{f}} \right) \tag{4}$$

where $Re(z,t) = Q(z,t)\phi/\nu A_r$ is the Reynolds number, ν is the kinematic viscosity (m²/s) and ε is the pipe's effective roughness height (m). However, since the Colebrook equation (4) is implicit for f , it has to be solved by using iterative methods which causes serious difficulties in repetitive calculations of the friction factor

such as those encountered in leak diagnostic algorithms. Because of this reason, over time a large number of studies developed several explicit approximations to the implicit Colebrook equation [31], [32].

Among the explicit approximations to the Colebrook equation available, in the present work, it was chosen to compute the friction factor by a power-law type equation as follows, [33]:

$$f(\text{Re}) = 0.4133 \left(\frac{\varepsilon}{\phi} \right) + 0.1110 \left(\frac{\varepsilon}{\phi} \right)^{0.2598} + 42.6463 \left(\frac{\varepsilon}{\phi} \right)^{0.3273} \text{Re}^{-1.3624 \left(\frac{\varepsilon}{\phi} \right)^{0.1124}} \quad (5)$$

The estimated error of this approximation is less than 10% in the range $104 < \text{Re} < 108$ and $2.25 \times 10^{-6} < \varepsilon/\phi < 10^{-1}$. Although this estimated error is greater than that obtained with other approximations [31], the convenience of using a power-law type equation will be explained in the next lines.

2.3 Liénard-type model for pipelines

Among dynamical systems and differential equations, a Liénard system [12] is a second-order differential equation given by

$$\ddot{x}(t) + F_0(x(t))\dot{x}(t) + G_0(x(t)) = 0 \quad (6)$$

where $\dot{x}(t) = dx(t)/dt$, $\ddot{x}(t) = d^2x(t)/dt^2$ for given functions F_0, G_0 , and a scalar variable $x(t)$. By the application of the following change of variable [34]

$$\begin{aligned} \zeta_1(t) &= x(t) \\ \zeta_2(t) &= \dot{x}(t) + F(x(t)) \end{aligned} \quad (7)$$

where $F(x) = \int_0^x F_0(\sigma) d\sigma$, the Liénard equation (6) can be rewritten in a state-space form as follows:

$$\begin{aligned} \dot{\zeta}_1(t) &= \zeta_2(t) - F(\zeta_1(t)) \\ \dot{\zeta}_2(t) &= -G_0(\zeta_1(t)). \end{aligned} \quad (8)$$

Representation (8) is called the Liénard form.

Furthermore, a representation only in terms of the flow rate can be obtained from (1) and (2), first, by differentiating (2) with respect to z as follows

$$\frac{\partial^2 H(z,t)}{\partial z \partial t} = -\frac{b^2}{gA_r} \frac{\partial^2 Q(z,t)}{\partial z^2}. \quad (9)$$

Then, by differentiating (1) with respect to t , we get

$$\frac{\partial^2 Q(z,t)}{\partial t^2} + gA_r \frac{\partial^2 H(z,t)}{\partial t \partial z} + \frac{|Q(z,t)|}{\phi A_r} \left[f(Q(z,t)) + \frac{Q(z,t)}{2} \frac{\partial f(Q(z,t))}{\partial Q} \right] \frac{\partial Q(z,t)}{\partial t} = 0. \quad (10)$$

By combining (9) and (10), we obtain:

$$\frac{\partial^2 Q(z,t)}{\partial t^2} + \frac{|Q(z,t)|}{\phi A_r} \left[f(Q(z,t)) + \frac{Q(z,t)}{2} \frac{\partial f(Q(z,t))}{\partial Q} \right] \frac{\partial Q(z,t)}{\partial t} - b^2 \frac{\partial^2 Q(z,t)}{\partial z^2} = 0, \quad (11)$$

which has the form of (6) with

$$\begin{aligned} F_0(Q(z,t)) &= \frac{|Q(z,t)|}{\phi A_r} \left[f(Q(z,t)) + \frac{Q(z,t)}{2} \frac{\partial f(Q(z,t))}{\partial Q} \right] \\ G_0(Q(z,t)) &= -b^2 \frac{\partial^2 Q(z,t)}{\partial z^2} \end{aligned} \quad (12)$$

Therefore, by considering the state variables definition in (7), that is $Q^a(z,t) = Q(z,t)$ and $Q^b(z,t) = \partial Q(z,t)/\partial t + F(x(t))$, (11) can be rewrite in a state-space form as follows:

$$\begin{aligned} \frac{\partial Q^a(z,t)}{\partial t} &= Q^b(z,t) - F(Q^a(z,t)) \\ \frac{\partial Q^b(z,t)}{\partial t} &= b^2 \frac{\partial^2 Q^a(z,t)}{\partial z^2} \end{aligned} \quad (13)$$

where $F(Q^a(z,t)) = \int_0^{Q^a(z,t)} F_0(\sigma) d\sigma$ and $F_0(\sigma)$ is given by the first equation in (12), Notice that $Q^a(z,t)$ is the flow rate flowing through the pipeline, while $Q^b(z,t)$ is proportional to the flow acceleration. The boundary conditions considered in this work to approximate (13) are the flow rates' behavior at the ends of the pipeline: $Q_{in}(t)$ and $Q_{out}(t)$.

Most of the explicit approximations to the Colebrook relation for flow friction are logarithmic functions [31], which makes difficult the calculation of $F(Q^a(z,t))$ in (13). This is a reason why an approximation with a simpler structure as in (5) becomes convenient in some cases such as in the design of fault detection methodologies based on mathematical models. Then, by considering (5), $F(Q^a(z,t))$ in (13) can be expressed as

$$F(Q^a(z,t)) = \frac{Q^a(z,t)|Q^a(z,t)|}{2000\phi A} \left[410 \left(\frac{\varepsilon}{\phi} \right) + 111 \left(\frac{\varepsilon}{\phi} \right)^{\frac{13}{50}} \right] - \frac{43Q^a(z,t)|Q^a(z,t)| \left(\frac{\varepsilon}{\phi} \right)^{\frac{33}{100}}}{2\phi^{(1+\kappa)} A_r \left(\frac{Q^a(z,t)}{\nu A} \right)^\kappa} \quad (14)$$

$$\text{with } \kappa = 34 \left(\frac{\varepsilon}{\phi} \right)^{\frac{14}{125}} / 25.$$

2.4 Space discretized Liénard-type model

On the off chance that (13) is spatial-discretized by utilizing the finite difference technique, it is obtained the lumped model:

$$\begin{aligned} \dot{Q}_i^a(t) &= Q_i^b(t) - F(Q_i^a(t)), \quad i = 1, 2, \dots, n_i \\ \dot{Q}_i^b(t) &= b^2 \left[\frac{Q_{i-1}^a(t) - 2Q_i^a(t) + Q_{i+1}^a(t)}{(\Delta z_i)^2} \right] \end{aligned} \quad (15)$$

where $Q^a(z,t)$ is the internal discrete flow of section i , $F(Q^a(z,t))$ is calculated through (14), $n_l+1=N_l$ is the total number of sections in which the pipeline has been spatially divided, and thus the spatial step is $\Delta z_i = L/N_l$ (see Fig 2).

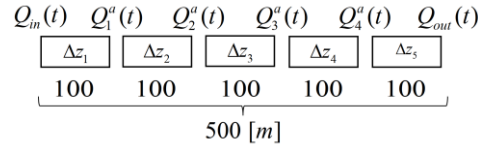


Figure 2. Space discretization schema.

Since in practice inlet and outlet flow rates ($Q_{in}(t)$ and $Q_{out}(t)$) are typically measured, it is consistent with using them as boundary conditions to calculate a numerical solution of (15). To avoid numerical issues, initial conditions $Q_i^a(z,0)$ must be set near to the expected nominal flow, and $Q_i^b(z,0)$ can be obtained from (7) by assuming a steady-state condition, that is $Q_i^b(z,0) = F(Q_i^a(z,0))$.

3. Monitoring approach

The strategy of our methodology incorporates a principal component analysis stage to detect a leak occurrence. PCA is a dimensionality reduction technique commonly used for fault detection that uses a linear orthogonal transformation to produce a set of values of linearly uncorrelated variables called principal components, from a given set of observations of possibly correlated variables [35]. Conventional PCA is shortly presented below.

3.1 Principal component analysis

For a better understanding, a block diagram of the PCA algorithm is showed in Fig 3. Notice that principal component analysis can be divided into two stages: an offline stage and an online stage. Data corresponding to process normal operation are arranged in a matrix $X^p \in \mathbb{R}^{n \times m}$, where each of the m columns represents a process variable being measured, and each of the n rows represents a different sample. It is important to address that variables with missing signal problems or with null variance must be excluded from matrix X^p .

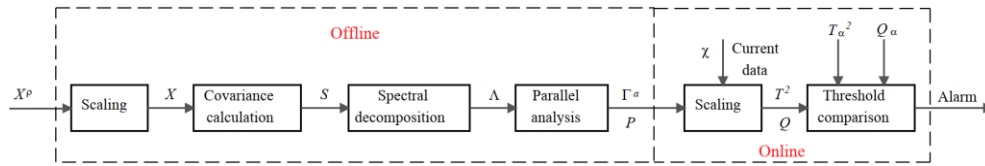


Figure 3. Principal components analysis block diagram.

Since the range of values of raw data may vary widely, it is very important to perform a data normalization (scaling) to standardize the range of the variables considered. Scaling is performed as follows

$$X = (X^p - I_n \mu) \Sigma^{-1} \quad (16)$$

where $\mu = (X^p)^T I_n / n$ is a vector containing the means of the m variables in X^p , $I_n = [1 \ 1 \ \dots \ 1] \in \mathbb{R}^n$ and $\sigma = \text{diag}(\sigma_1, \sigma_2, \dots, \sigma_m)$ is a diagonal matrix containing the standard deviations of the m variables in X^p . Once the data are normalized spectral decomposition of the covariance matrix $S = X^T X / (n-1)$ is calculated as follows

$$S = V \Lambda V^T \quad (17)$$

where Λ is an $m \times m$ diagonal matrix containing the non-negative real eigenvalues arranged in descending order along its main diagonal, and V is an $m \times m$ matrix containing the corresponding eigenvectors. After that, the statistics T^2 and Q are calculated as follows [36]

$$\begin{aligned} T^2 &= \chi^T P \Gamma_a^{-2} P^T \chi \\ Q &= \chi^T (1 - PP^T) \chi, \quad \chi \in \mathbb{R}^{1 \times m} \end{aligned} \quad (18)$$

where a is the number of principal components selected by using parallel analysis as a dimensional reduction technique [35], [37], $P \in \mathbb{R}^{m \times a}$ is the so-called loading matrix which contains the first a columns of V , the matrix $\Gamma_a \in \mathbb{R}^{a \times a}$ is composed of the first a rows and columns of Γ , which in turn is an $m \times m$ matrix such that $\Lambda = \Gamma^T \Gamma$.

3.2 Methodology description

Fig 4 shows a flow diagram of the proposed approach. The proposed methodology is founded on the model (15), assuming as inputs the inlet and outlet flow rates $Q_{in}(t)$ and $Q_{out}(t)$. Given the spatial discretization of the model (15), this lets us calculate the flow rate for each section in which the pipeline was divided. Unlike what happened when a leak takes place, in the absence of leaks all flow rates given by the model will be equivalent.

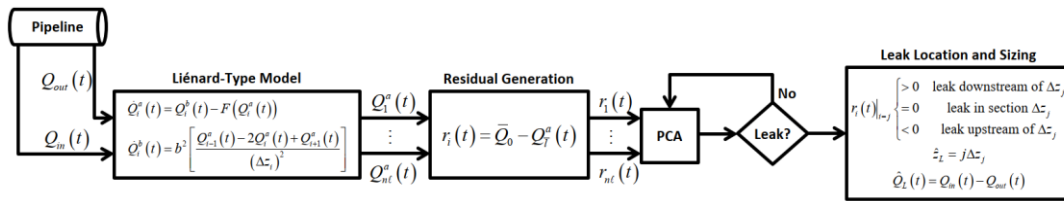


Figure 4. Methodology flow diagram.

The difference between the flow rate observed for the section i and the mean flow rate of the pipeline without leaks $Q_0(t)$, is the i -th residual and is given by

$$r_i(t) = Q_0(t) - Q_i^a(t), \quad \forall i = 1, 2, \dots, n_l, \quad \forall l' = n_l, n_l - 1, \dots, 1. \quad (19)$$

The residuals are used to feed a principal component analysis algorithm to detect a leak occurrence. Whenever a leak is detected, the section where the leak occurs can be determined from the analysis of the behavior of the residuals as follows:

$$r_j(t) \begin{cases} > 0, & \text{if the leak is downstream of } \Delta z_j; \\ \approx 0, & \text{if the leak is in section } \Delta z_j; \\ < 0, & \text{if the leak is upstream of section } j. \end{cases} \quad (20)$$

Once j (the section number where the leak occurs) is determined, the position of the leak is calculated as follows

$$z'_L = j \Delta z_j. \quad (21)$$

When a leak takes place, a mass balance is used to calculate the leak amount, that is

$$Q'_L(t) = Q_{in}(t) - Q_{out}(t). \quad (22)$$

However, if once a leak has occurred, others M leaks occur sequentially, the first leak amount is calculated by (22), and each subsequent flow is computed by as follows

$$Q'_{eq}(t) = \sum_{k=1}^M Q'_{L_k} \quad (23)$$

where $Q'_{eq}(t)$ is the total leak amount (equivalent leak flow), and $Q'_{L_k}(t)$ is the leak amount of the k -th sequential leak. The position associated with the equivalent leak flow, let's call it the equivalent position z'_{eq} , will be indicated by the residual closets to zero. And the location of the k -th sequential leak z'_{L_k} , can be calculated by

$$z'_{eq} Q'_{eq}(t) = \sum_{k=1}^M Q'_{L_k}(t) z'_{L_k} \quad (24)$$

4. Application results

Two scenarios regarding the application of the proposed method algorithms are presented. The first one is simulation-based, while in the second one real data obtained from a laboratory pipeline is used.

4.1 Simulation test

In this section, the dynamic behavior of water at 30°C flowing through a horizontal pipe was recreated with the industrial pipeline software PipelineStudio®. Below are presented the results of two simulation-based tests in a horizontal pipeline through which water flows at 30°C: 1) the single leaks case and 2) the sequential leaks case.

- **Test 1:** In this case, a three single independent leaks scenario is considered for a pipeline with the characteristic shown in Table 2.

Table 2. Test 1 pipeline physical parameters.

Symbol	Value	Units	Description
g	9.81	m/s ²	Gravitational acceleration
L	170	m	Pipeline length
ϕ	0.1016	m	Pipeline diameter
ε	1.83×10^{-3}	m	Mean height of roughness
ν	7.9822×10^{-7}	m ² /s	Kinematic viscosity

The three independent single leak were induced at $z_{L1} = 15$ (m), $z_{L2} = 90$ (m) and $z_{L3} = 146$ (m). The leaks were activated at the instants $t_{L1} = 100$ (s), $t_{L2} = 300$ (s) and $t_{L3} = 500$ (s) and each one had a duration of 100 (s). The mean values of the boundary conditions considered were $H_{in}(t) = 20$ (m) and $H_{out}(t) = 4$ (m). Fig 5 shows upstream, and downstream pressure heads injected to the PipelineStudio® simulator, and the flow rates provided by this for the leaks scenario considered. Notice that the mean nominal flow obtained was about $Q_0 = 0.0279$ (m³/s).

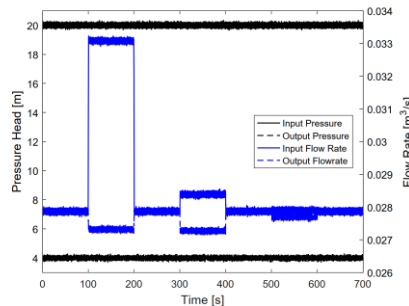


Figure 5. Simulation test 1. Pressures and flow rates at the pipeline ends.

On the other hand, Fig 6(a) shows the discrete flows computed by the Liénard-type model (15) with $\Delta z_i = L/N_i = 170/21 = 8.1$ (m), and Fig 6(b) shows the residuals calculated through (19) for each of the leaks considered.

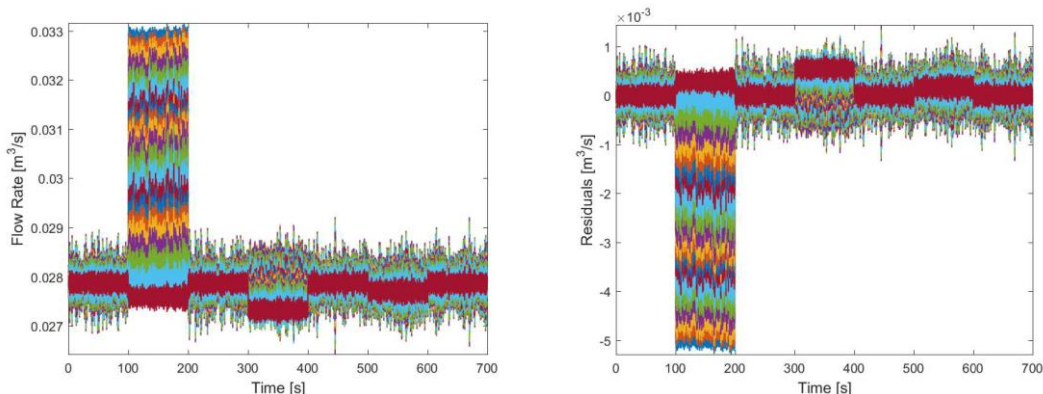


Figure 6. Simulation test 1. (a) Discrete flows and (b) Residuals.

The effects of the leak on the synthetic flows are observed (once a leak occurs the leak outflow is distributed as several leaks in each discretization node). Fig 7(a) shows the response of Hotelling’s statistic and the results of leak position and leak flow rate estimations are showed in Fig 7(b).

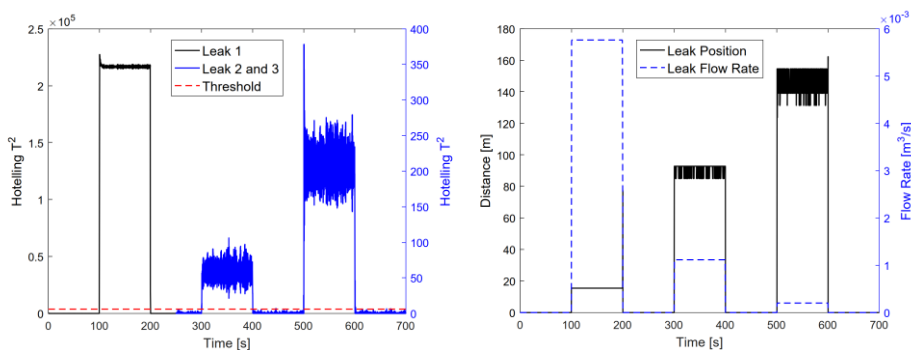


Figure 7. Simulation test 1. (a) Hotelling’s T^2 statistic and (b) Estimated leak position and leak flow rate.

The residuals with mean value closets to zero were $r_2(t)$, $r_{12}(t)$, and $r_{19}(t)$ for the leaks 1, 2, and 3 respectively. The leak positions were estimated through (21). Table 3 summarizes the estimated leak positions z'_L and the estimation errors obtained for each one of three leaks considered. The estimation errors were calculated as $e = 100|(z_L - z'_L)/L|$. It is important to address that the minimal leak detectable corresponds to a flow rate of 2×10^{-4} (m^3/s) (leak 3), which is equivalent to 0.72% of the nominal flow.

Table 3. Simulation Test - Single Leaks Diagnosis Results.

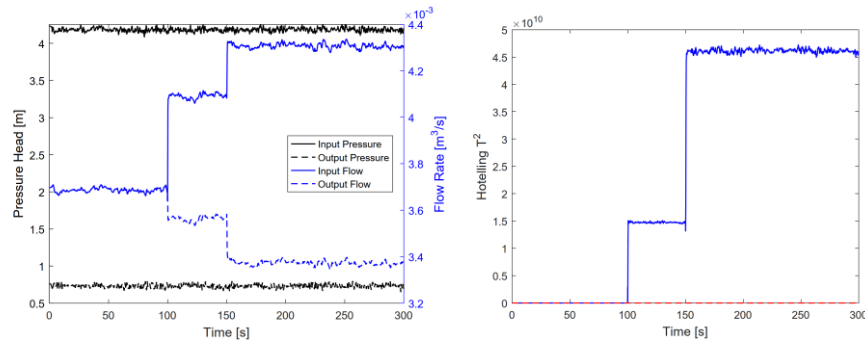
z_L (m)	z'_L (m)	Error (%)
15	15.45	0.27
90	92.73	1.6
146	146.82	0.48

- **Test 2:** In this case, a two sequential leaks scenario is considered for a pipeline characterized by the parameters shows in Table 4.

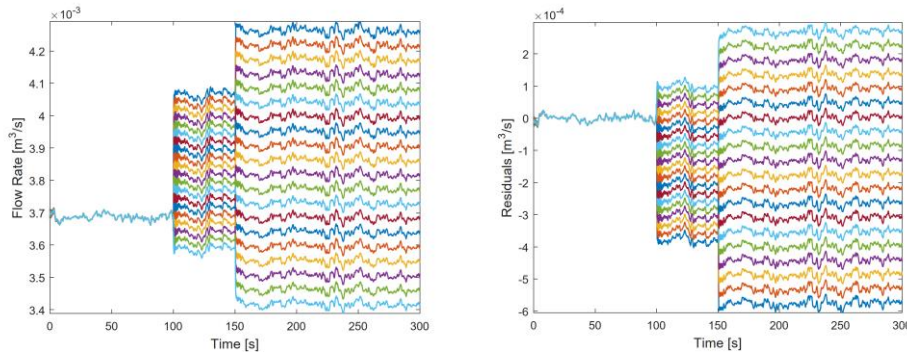
Table 4. Test 2 Pipeline Physical Parameters.

Symbol	Value	Units	Description
g	9.81	m/s^2	Gravitational acceleration
L	57.76	m	Pipeline length
ϕ	0.052	m	Pipeline diameter
ε	1.654×10^{-5}	m	Mean height of roughness
ν	8.0066×10^{-7}	m^2/s	Kinematic viscosity

The two sequential leaks were induced at position $z_{L1} = 12.87$ (m) and $z_{L2} = 25.3$ (m), at the instants $t_{L1} = 100$ (s) and $t_{L2} = 150$ (s). The mean values of the boundary conditions considered were $H_{in}(t) = 4.18$ (m) and $H_{out}(t) = 0.73$ (m). Fig 8(a) shows upstream and downstream pressure heads injected to the PipelineStudio® simulator and the flow rates provided by this for the two sequential leaks considered, and Fig 8(b) shows the response of Hotelling's statistic.


Figure 8. Simulation test 2. (a) Pressures and flow rates and (b) Hotelling's T2 statistic.

The discrete flows computed by the Liénard-type model (15), with $\Delta z_i = L/N_i = 57.76/21 = 2.75$ (m), are shown in Fig 9(a), and the residuals in Fig 9(b).


Figure 9. Simulation test 2. (a) Discrete flows and (b) Residuals.

Through the equation (22) the flow of the first leak is obtained, $Q'_{L1} = 5.3 \times 10^{-4}$ (m^3/s). Once the second leak occurs, the same equation is used to calculate the equivalent leak flow, $Q'_{eq} = 9.4 \times 10^{-4}$ (m^3/s). At this point, the equation (23) is used to obtain the flow of the second leak, $Q'_{L2} = 4.1 \times 10^{-4}$ (m^3/s). It can be verified that residuals with mean value closets to zero are $r_5(t)$ and $r_7(t)$ before and after the second leak respectively (see Fig 9). Consequently, $z'_{L1} = 5\Delta z_i = 13.75$ (m) and $z'_{eq} = 7\Delta z_i = 19.25$ (m). The equation (24) allows calculating the position of the second leak, $z'_{L2} = 26.36$ (m). Table 5 summarizes the estimated leak positions z'_L and the estimation errors obtained in this case.

Table 5. Simulation Test - Sequential Leaks Diagnosis Results.

z'_L (m)	z''_L (m)	Error [%]
12.87	13.75	1.55
25.3	26.36	1.87

4.2 Experimental test

In this section, some experimental test results are presented. The diagnosis of two single leaks is performed. Flow rates measurements at the ends of a pipeline prototype built in Instituto Tecnológico de Tuxtla Gutiérrez are used as a boundary condition to the Liénard-type model (15) Table 4 provides the list of model parameters considered. The prototype considered here (Fig 10) is equipped with:

- A 5 (HP) centrifugal pump, which provides the energy needed to recirculate the water from a reservoir through a PVC pipeline of 0.052 (m) of diameter and 57.76 (m) of length.
- A Siemens Micromaster 420 variable-frequency drive which controls the rotational speed of the pump motor by a variation of the AC frequency in a range from 0 to 60 (Hz).
- Four valves to emulate leaks.
- Flow and pressure sensors installed at both ends of the pipeline.

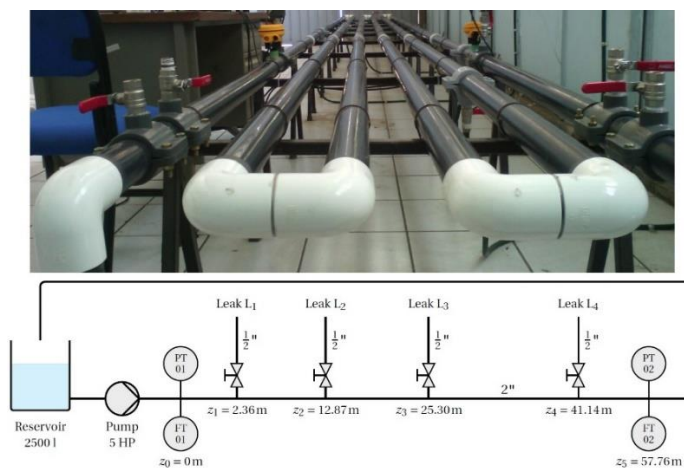


Figure 10. Pipeline prototype for experimental test.

Then, in this case, two independent single leak cases were induced at $z_{L1} = 12.87$ (m) and $z_{L2} = 25.3$ (m). The leaks were activated at the instant $t_{L1} = 115$ (s) and $t_{L2} = 120$ (s) respectively. Fig 11(a) and Fig 11(b) show upstream and downstream pressure heads and input and output flow rates for both leak 1 and leak 2 respectively. Notice that the nominal mean flows obtained were about 4.85×10^{-3} (m³/s) and 4.68×10^{-3} (m³/s) for leaks 1 and 2 respectively.

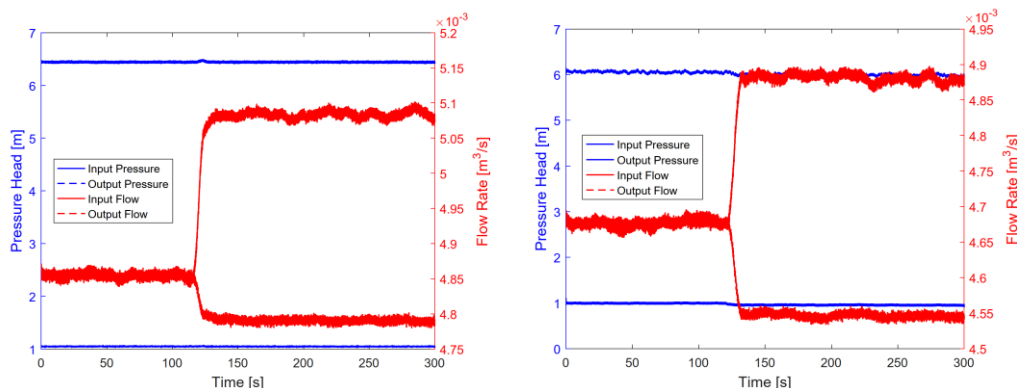


Figure 11. Experimental Test. Pressures and flow rates at the pipeline ends (a) Leak 1 and (b) Leak 2.

Similarly to the simulation tests, the Liénard-type model (15) was programmed in MATLAB® with a space step $\Delta z_i = L/N_i = 57.76/22 = 2.63$ (m). Fig 12(a) and Fig 12(b) shows the residuals calculated through (19) for the leaks 1 and 2 respectively. The residuals with mean value closets to zero were $r_5(t)$ and $r_9(t)$ for the leaks 1 and 2 respectively. The leak positions were estimated through (21). Table 6 summarizes the estimated leak positions and the estimation errors obtained for each one of two leaks considered.

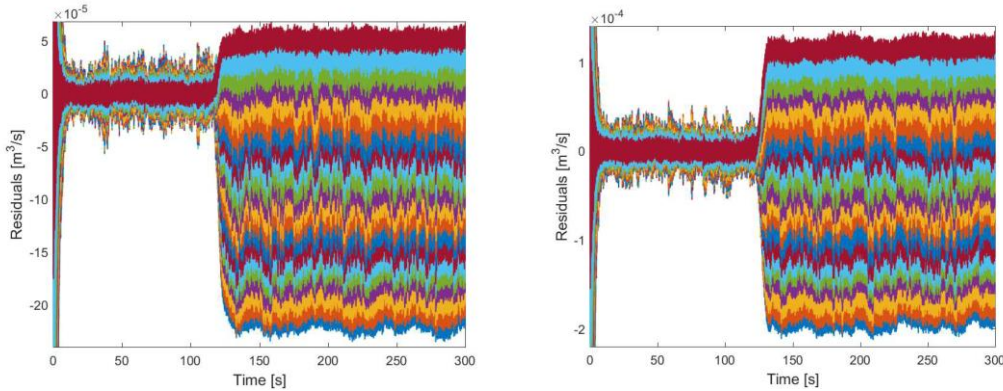


Figure 12. Experimental test residuals. (a) Leak 1 and (b) Leak 2.

Table 6. Experimental test. Single leaks diagnosis results.

z_L (m)	z'_L (m)	Error [%]
12.87	13.3	0.45
25.3	23.13	2.89

5. Conclusions

In this paper presents a novel non-invasive approach that allows diagnoses single and sequential leaks. To avoid the necessity of using pressure measurements, a representation of the pipeline dynamics under the form of a Liénard equation was used for the formulation of the proposed method. Since flow-rate sensors are commonly available at the ends of the pipelines together with pressure sensors, the proposed approach can be used as a backup system in the case that some pressure sensor fails. Provided simulations and, even more importantly, experimental tests illustrated the good leak position estimation results obtained with the proposed methodology. Maximum estimation errors for the leak position of 3.8% and 2.89% in simulation and experimental tests respectively were obtained. Tests in real-life scenarios, in which assumptions such as a constant cross-section area and a constant roughness height might not be valid, are envisaged as part of our future research.

6. References

- [1] R. P. API, “1130: Computational Pipeline Monitoring for Liquids.” American petroleum institute, 2007.
- [2] C. Sandberg, J. Holmes, K. McCoy, and H. Koppitsch, “The application of a continuous leak detection system to pipelines and associated equipment,” *IEEE Trans. Ind. Appl.*, vol. 25, no. 5, pp. 906–909, 1989.
- [3] W. J. Reddy III, “Capacitance measuring circuit and method for liquid leak detection by measuring charging time.” Google Patents, 1992.
- [4] R. K. Miller *et al.*, “The development of acoustic emission for leak detection and location in liquid-filled, buried pipelines,” in *Acoustic Emission: Standards and Technology Update*, ASTM International, 1999.

- [5] J. Campuzano-Cervantes, F. Meléndez-Pertuz, B. Núñez-Perez, and J. Simancas-García, “Sistema de Monitoreo Electrónico de Desplazamiento de Tubos de Extensión para Junta Expansiva,” *Rev. Iberoam. Automática e Informática Ind. RIAI*, vol. 14, no. 3, pp. 268–278, 2017.
- [6] S. R. Reddy, “System and method for detecting leaks in a vapor handling system.” Google Patents, 1993.
- [7] V. V Spirin, M. G. Shlyagin, S. V Miridonov, F. J. M. Jimenez, and R. M. L. Gutierrez, “Fiber Bragg grating sensor for petroleum hydrocarbon leak detection,” *Opt. Lasers Eng.*, vol. 32, no. 5, pp. 497–503, 1999.
- [8] N. Kasai, C. Tsuchiya, T. Fukuda, K. Sekine, T. Sano, and T. Takehana, “Propane gas leak detection by infrared absorption using carbon infrared emitter and infrared camera,” *NDT E Int.*, vol. 44, no. 1, pp. 57–60, 2011.
- [9] C. Verde, “Multi-leak detection and isolation in fluid pipelines,” *Control Eng. Pract.*, vol. 9, no. 6, pp. 673–682, 2001.
- [10] L. Torres, G. Besançon, and D. Georges, “A collocation model for water-hammer dynamics with application to leak detection,” in *Decision and Control, 2008. CDC 2008. 47th IEEE Conference on*, 2008, pp. 3890–3894, doi: 10.1109/CDC.2008.4739304.
- [11] S. Verde, Cristina and Visairo, Nancy and Gentil, “Two leaks Isolation in a pipeline by transient response,” *Adv. Water Resour.*, vol. 30, no. 8, pp. 1711–1721, 2007.
- [12] J. Jiménez, L. Torres, I. Rubio, and M. Sanjuan, “Auxiliary Signal Design and Liénard-type Models for Identifying Pipeline Parameters,” in *Modeling and Monitoring of Pipelines and Networks*, Springer, 2017, pp. 99–124.
- [13] J. Jiménez, L. Torres, C. Verde, and M. Sanjuán, “Friction estimation of pipelines with extractions by using state observers,” *IFAC-PapersOnLine*, vol. 50, no. 1, pp. 5361–5366, 2017.
- [14] N. R. Bellahsene, M. Mostefai, and E. K. A. Oum, “Extended Kalman observer based sensor fault detection,” *Int. J. Electr. Comput. Eng. (2088- 8708)*, vol. 9, no. 3, 2019.
- [15] M. Brunone, Bruno and Ferrante, “Detecting leaks in pressurised pipes by means of transients,” *J. Hydraul. Res.*, vol. 39, no. 5, pp. 539–547, 2001.
- [16] B. W. Colombo, Andrew F and Lee, Pedro and Karney, “A selective literature review of transient-based leak detection methods,” *J. Hydro-environment Res.*, vol. 2, no. 4, pp. 212–227, 2009.
- [17] U.S. Department of Transportation, “Pipeline and Hazardous Materials Safety Administration: Pipeline Significant Incident 20 Year Trend.” 2019.
- [18] J. C. P. Liou, “Leak detection by mass balance effective for Norman wells line,” *Oil gas J.*, vol. 94, no. 17, 1996.
- [19] J. C. P. Lion, “Leak Detection: A Transient Flow Simulation Approach,” in *Pipeline Engineering AME Petroleum Division Publication PD V60, 1994 Proceedings of the Energy Source Technology Conference*, 1995.
- [20] P. Ostapkowicz, “Leak detection in liquid transmission pipelines using simplified pressure analysis techniques employing a minimum of standard and non-standard measuring devices,” *Eng. Struct.*, vol. 113, pp. 194–205, 2016.
- [21] R. A. Silva, C. M. Buiatti, S. L. Cruz, and J. A. F. R. Pereira, “Pressure wave behaviour and leak detection in pipelines,” *Comput. Chem. Eng.*, vol. 20, pp. S491–S496, 1996.
- [22] E. Farmer, “System for monitoring pipelines.” Google Patents, 1989.
- [23] R. Isermann, “Process fault detection based on modeling and estimation methods-A survey,” *automatica*, vol. 20, no. 4, pp. 387–404, 1984.
- [24] L. Billmann and R. Isermann, “Leak detection methods for pipelines,” *Automatica*, vol. 23, no. 3, pp. 381–385, 1987.
- [25] L. Torres, G. Besançon, and C. Verde, “Liénard type model of fluid flow in pipelines: Application to estimation,” in *12th International Conference on Electrical Engineering, Computing Science and Automatic Control (CCE)*, 2015, pp. 1–6.
- [26] L. Torres, J. A. D. Aguiñaga, G. Besançon, C. Verde, and O. Begovich, “Equivalent Liénard-type models for a fluid transmission line,” *Comptes Rendus Mécanique*, 2016.
- [27] M. H. Chaudhry, *Applied Hydraulic Transients*. Springer New York, 2013.
- [28] J. Jimenez Cabas and J. D. Ruiz Ariza, “Modeling and Simulation of a Pipeline Transportation Process,” vol. 13, no. 9, 2018.

- [29] A. C. Yunus and J. M. Cimbala, “Fluid mechanics fundamentals and applications,” *McGraw-Hill Publ.*, 2006.
- [30] L. F. Moody, “Friction factors for pipe flow,” *Trans Asme*, vol. 66, pp. 671–684, 1944.
- [31] D. Brkić, “Review of explicit approximations to the Colebrook relation for flow friction,” *J. Pet. Sci. Eng.*, vol. 77, no. 1, pp. 34–48, 2011.
- [32] J. Jiménez, L. Torres, C. Verde, and M. Sanjuán, “Friction estimation of pipelines with extractions by using state observers,” *IFAC-PapersOnLine*, vol. 50, no. 1, 2017, doi: 10.1016/j.ifacol.2017.08.942.
- [33] J. Jiménez-Cabas, E. Romero-Fandiño, L. Torres, M. Sanjuan, and F. R. López-Estrada, “Localization of Leaks in Water Distribution Networks using Flow Readings,” *IFAC-PapersOnLine*, vol. 51, no. 24, pp. 922–928, 2018.
- [34] L. Torres, J. A. D. Aguiñaga, G. Besançon, C. Verde, and O. Begovich, “Equivalent Li{é}nard-type models for a fluid transmission line,” *Comptes Rendus M{é}canique*, vol. 344, no. 8, pp. 582–595, 2016.
- [35] I. Portnoy, K. Melendez, H. Pinzon, and M. Sanjuan, “An improved weighted recursive PCA algorithm for adaptive fault detection,” *Control Eng. Pract.*, vol. 50, pp. 69–83, 2016.
- [36] J. E. Jackson and G. S. Mudholkar, “Control procedures for residuals associated with principal component analysis,” *Technometrics*, vol. 21, no. 3, pp. 341–349, 1979.
- [37] W. R. Zwick and W. F. Velicer, “Comparison of five rules for determining the number of components to retain,” *Psychol. Bull.*, vol. 99, no. 3, p. 432, 1986.